Generation of Arbitrarily-Oriented Ripple Images Using Circular-Sector-Type Smoothing Filter and Inverse Filter

Toru Hiraoka
Department of Information Systems, University of Nagasaki,
1-1-1, Manabino Nagayo, Nishisonogi, Nagasaki, 815-2195, Japan
E-mail: hiraoka@sun.ac.jp

Abstract

A non-photorealistic rendering (NPR) method for generating ripple images from photographic images has been proposed using intensity gradient. Ripple patterns imitate a wave on the water surface and are composed of continuous lines with fluctuations. Ripple images are expressed by superimposing ripple patterns on photographic images. However, the conventional method can only generate vertical and horizontal ripple patterns. Therefore, in this paper, we develop a method that can generate ripple patterns in any orientation. Ripple images generated by the proposed method are called arbitrarily-oriented ripple (AOR) images. The proposed method is executed by an iterative process using circular-sector-type smoothing filter and inverse filter. To verify the effectiveness of our method, we investigate the changes in AOR images by changing the values of the parameters.

Keywords: non-photorealistic rendering, ripple pattern, arbitrarily orientation, circular-sector-type smoothing filter, inverse filter

1. Introduction

NPR is a technology of computer graphics that can generate effective illustrations and artistic images. Many NPR methods have been proposed to simulate effective illustrations and artistic images[1,2,3,4,5]. In the past NPR methods, an NPR method for generating ripple images has been proposed[6]. Ripple patterns imitate a wave on the water surface and are composed of continuous lines with fluctuations. Ripple images are expressed by superimposing ripple patterns on photographic images. The conventional method was conducted by an iteration process with intensity gradients. Although the conventional method can generate ripple patterns in horizontal and vertical orientations, it is not possible to generate ripple patterns with arbitrary slope.

In this paper, we develop a method that can arbitrarily change the orientation of ripple patterns, then expand the range of expression of the conventional method. Ripple images generated by the proposed method is called AOR images. The proposed method is executed by an iterative process using inverse filter[7,8] and circular-sector-type smoothing filter. By adjusting the value of the parameter in the proposed method, ripple patterns of the proposed method is more linear or wavy than ripple patterns of the conventional method. In addition, by changing the value of the parameter, the proposed method can also change the interval between ripple patterns as the conventional method. To verify the effectiveness of the proposed method, experiments are conducted using Lenna image and other photographic images. As a result of the experiments, it is clarified that the proposed method can automatically generate AOR images. In addition, through experiments that change the values of parameters in the proposed method, it is also revealed the changes in appearance of AOR images.

The rest of this paper is organized as follows. Section 2 describes the proposed method for generating AOR images. Section 3 shows experimental results, and reveals the effectiveness of the proposed method. Finally, Section 4 concludes this paper.

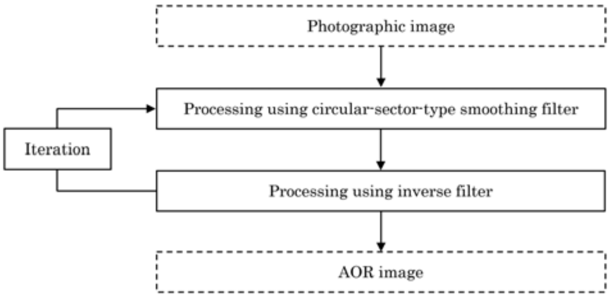

Fig. 1. Flow chart of the proposed method.

2. Proposed Method

The proposed method is executed in two processes. In the first process, images are smoothed using circular-sector-type smoothing filter. In the second process, the smoothed images are restored using inverse filter. By repeating the two processes, AOR images are generated. Accumulation of errors due to the iterative process is a factor that can generate ripple patterns. A flow chart of the proposed method is shown in Fig. 1. The detailed procedure in Fig. 1 is shown as follows.

The input pixel values for spatial coordinates (i, j) of a photographic image are defined as $f_{i,j}$. Then, the pixel values of the image at the t-th iteration number are defined as $f_{i,j}^{(t)}$, where $f_{i,j}^{(1)} = f_{i,j}$. The pixel values $f_{i,j}^{(t)}$ have value of M gradation from 0 to $M-1$.

In the first process, the image with the pixel values $f_{i,j}^{(t)}$ is smoothed using circular-sector-type smoothing filter that calculates an average of pixel values in circular sector as shown in Fig. 2. The circular sector with a range of θ_1 radian and radius D rotates θ_2 radian, and the pixel values that the center of the pixel is included in circular sector at the target pixel (i, j) are $g_{i,j,k}^{(t)}(k = 1,2,\cdots,K_{i,j}^{(t)})$. The pixel values $s_{i,j}^{(t)}$ of the smoothed image are calculated as the following equation.

$$s_{i,j}^{(t)} = \frac{\sum_{k=1}^{K_{i,j}^{(t)}} g_{i,j,k}^{(t)}}{K_{i,j}^{(t)}} \tag{1}$$

In the second process, the pixel values $f_{i,j}^{(t+1)}$ using inverse filtering are calculated as the following equation.

$$f_{i,j}^{(t+1)} = f_{i,j}^{(t)} - s_{i,j}^{(t)} + f_{i,j} \tag{2}$$

In case $f_{i,j}^{(t+1)}$ is less than 0, then $f_{i,j}^{(t+1)}$ must be set to 0. In case $f_{i,j}^{(t+1)}$ is greater than $M-1$, then $f_{i,j}^{(t+1)}$ must be set to $M-1$. An AOR image is obtained after the first and second processes of T times iteration.

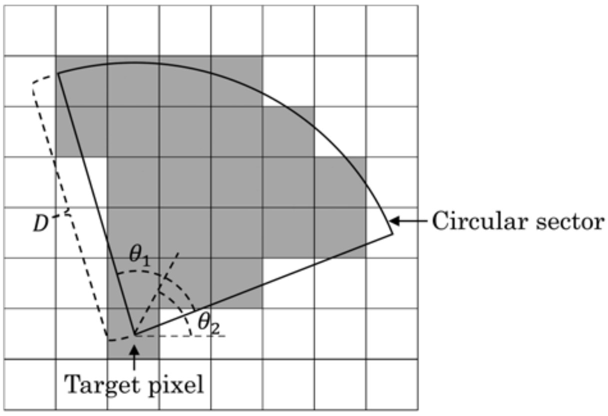

Fig. 2. Conceptual diagram of circular-sector-type smoothing filter.

Fig. 3. Lenna image.

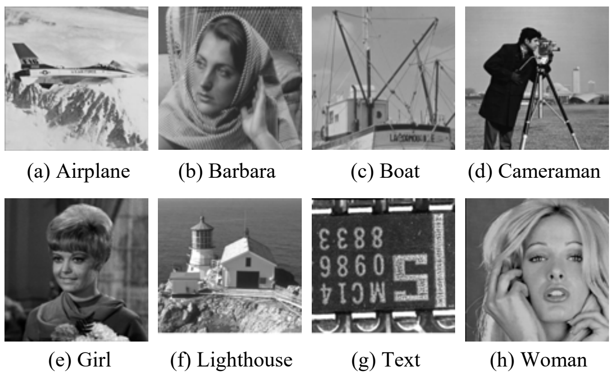

Fig. 4. Various photographic images.

3. Experiments

We mainly conducts two experiments. First, the experiment with changing the values of the parameters in the proposed method is conducted using Lenna image shown in Fig. 3. Second, the experiment is conducted to verify that patterns can be generated using various photographic images shown in Fig. 4. All photographic images used in the experiments are 512 * 512 pixels and 256 gradation.


(a) $T = 10$


(b) $T = 20$


(c) $T = 50$


(d) $T = 100$

Fig. 5. AOR images in the case of the iteration number $T = 10{,}20{,}50$, and 100.


(a) $D = 3$


(b) $D = 5$

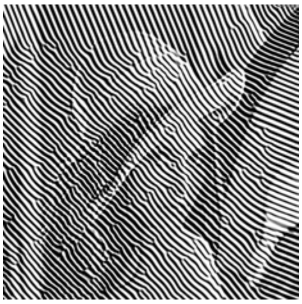
(c) $D = 7$


(d) $D = 9$

Fig. 6. AOR images in the case of the radius $D = 3{,}5{,}7$, and 9.

3.1. *Experiment with changing parameters*

AOR images by changing the iteration number T are visually confirmed using Lenna image. The iteration number T is set to 10, 20, 50, and 100. Other parameters D, θ_1, and θ_2 are set to 5, $\pi/2$, and $\pi/4$, respectively. The results of the experiment are shown in Fig. 5. As the value of the iteration number T is larger, ripple patterns become clear and converge.

AOR images by changing the radius D are visually confirmed using Lenna image. The radius D is set to 3, 5, 7, and 9. Other parameters T, θ_1, and θ_2 are set to 100, $\pi/2$, and $\pi/4$, respectively. The results of the experiment are shown in Fig. 6. As the value of the radius D is larger, the intervals between ripple patterns become wider.

AOR images by changing the angle θ_1 are visually confirmed using Lenna image. The angle θ_1 is set to $\pi/6$, $\pi/3$, $\pi/2$, and $(2/3)\pi$. Other parameters T, D, and θ_2 are set to 100, 5, and $\pi/4$, respectively. The results of the experiment are shown in Fig. 7. As the value of the angle θ_1 is larger, ripple patterns become more linear. On the other hand, as the value of the angle θ_1 is larger, ripple patterns become wavier.

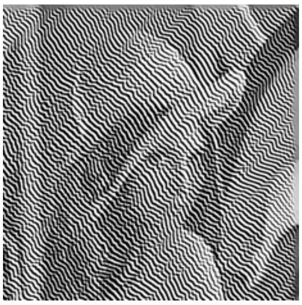
(a) $\theta_1 = \pi/6$

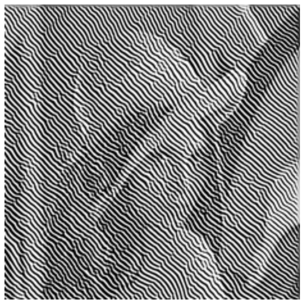
(b) $\theta_1 = \pi/3$


(c) $\theta_1 = \pi/2$


(d) $\theta_1 = (2/3)\pi$

Fig. 7. AOR images in the case of the angle $\theta_1 = \pi/6\,,\pi/3\,,\pi/2$, and $(2/3)\pi$.

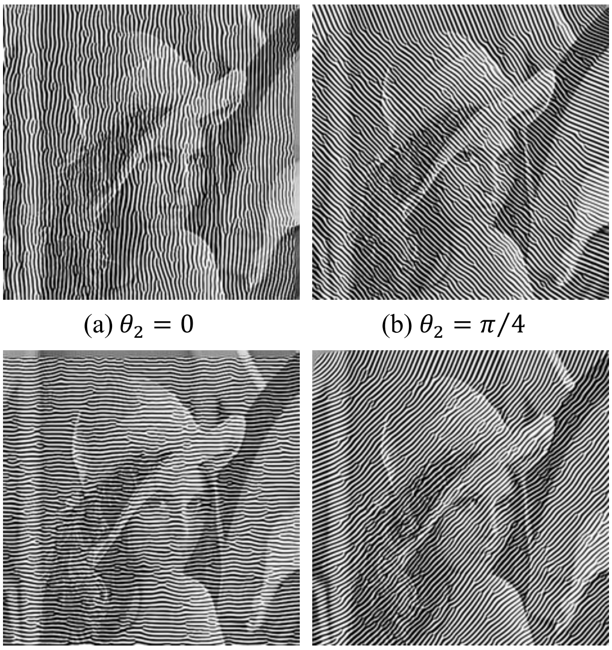

(a) $\theta_2 = 0$ (b) $\theta_2 = \pi/4$

(c) $\theta_2 = \pi/2$ (d) $\theta_2 = (3/4)\pi$

Fig. 8. AOR images in the case of the angle $\theta_1 = 0, \pi/4, \pi/2$, and $(3/4)\pi$.

AOR images by changing the angle θ_2 are visually confirmed using Lenna image. The angle θ_2 is set to 0, $\pi/4$, $\pi/2$, and $(3/4)\pi$. Other parameters T, D, and θ_1 are set to 100, 5, and $\pi/2$, respectively. The results of the experiment are shown in Fig. 8. Depending on the value of the angle θ_2, the orientation of ripple patterns is changing.

3.2. *Experiment using various photographic images*

The proposed method is applied to eight photographic images shown in Fig. 4. The parameters T, D, θ_1, and θ_2 are set to 100, 5, $\pi/2$, and $\pi/4$, respectively. The results of the experiment are shown in Fig. 9. In all cases, ripple patterns can be automatically generated on the whole image. However, no ripple patterns are generated in the white areas shown in Fig. 9 (f) and (g). It is conceivable to generate a ripple pattern by adding noise to the white area.

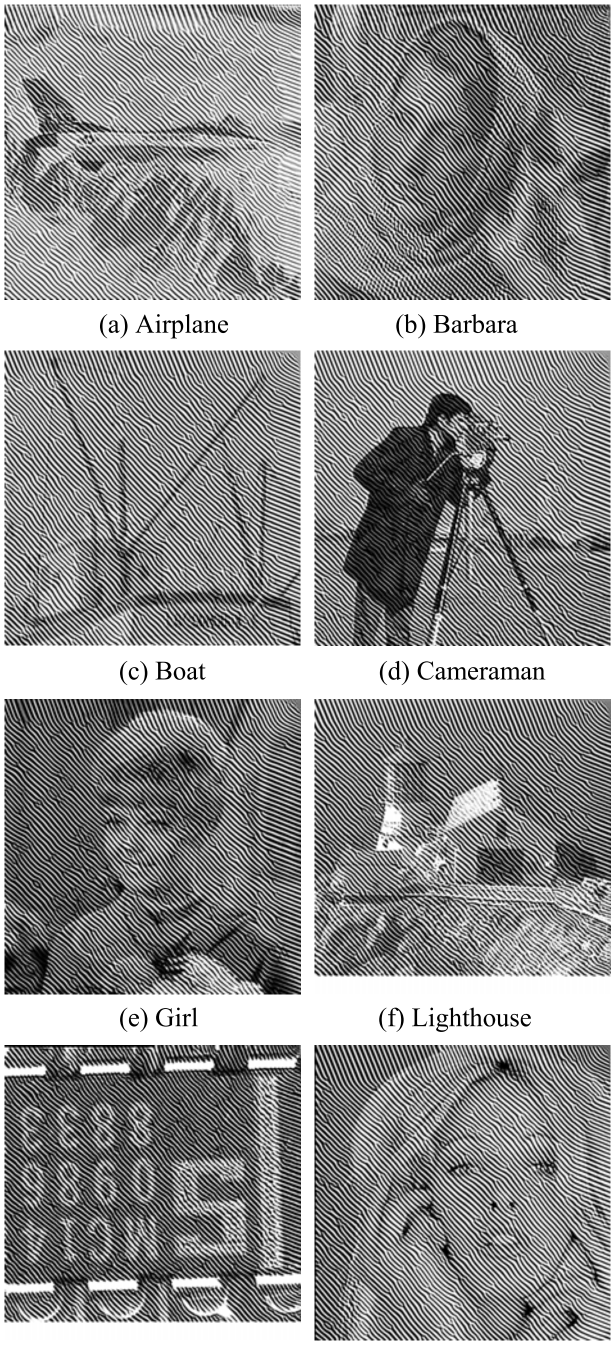

(a) Airplane (b) Barbara

(c) Boat (d) Cameraman

(e) Girl (f) Lighthouse

(g) Text (h) Woman

Fig. 9. AOR images.

4. Conclusion

We proposed an NPR method for generating AOR images from photographic images. The proposed method was executed by an iterative process using inverse filter and circular-sector-type smoothing filter. To verify the effectiveness of the proposed method, the changes in AOR images by changing the values of the parameters were investigated. As a result of the experiments, by changing the value of the angle θ_2 in the proposed method, ripple patterns could be generated in any orientation. And, by changing the value of the angel θ_1, ripple patterns could be generated more linear or wavy. And, by changing the value of the radius D, the proposed method could also change the interval between ripple patterns.

A subject for future study is to expand the proposed method for application to color photographic images and videos.

Acknowledgements

This work was supported by JSPS KAKENHI Grant Number JP19K12664.

References

1. P. Haeberli, Paint by numbers: abstract image representations, *ACM SIGGRAPH Computer Graphics.* **24**(4), 1990, pp. 207-214.
2. D. D. Seligmann and S. Feiner, Automated generation of intent-based 3D illustrations, *ACM SIGGRAPH Computer Graphics.* **25**(4), 1991, pp. 123-132.
3. W. Qian, D. Xu, K. Yue, Z. Guan, Y. Pu and Y. Shi, Gourd pyrography art simulating based on non-photorealistic rendering, *Multimedia Tools and Applications.* **76**(13), 2017, pp. 14559-14579.
4. D. Martin, G. Arroyo, A. Rodriguez and T. Isenberg, A survey of digital stippling, *Computers & Graphics.* **67**, 2017, pp. 24-44.
5. W. Qian, D. Xu, J. Cao, Z. Guan and Y. Pu, Aesthetic art simulation for embroidery style, *Multimedia Tools and Applications.* **78**(1), 2019, pp. 995-1016.
6. T. Hiraoka, Generation of ripple images using intensity gradient, *ICIC Express Letters.* **13**(1), 2019, pp. 1097-1101.
7. J. M. Ortega and W. C. Rheinboldt, Iterative solutions of nonlinear equations in several variables, *Society for Industrial Mathematic.* 1987.
8. Yu and K. Urahama, Iterative method for inverse nonlinear image processing, *IEICE Transactions on Fundamentals.* **E97-A**(2), 2014, pp. 719-72.